Peptide Structure

DOI: 10.1002/anie.201102887

A Membrane-Bound Antiparallel Dimer of Rat Islet Amyloid Polypeptide**

Abhinav Nath, Andrew D. Miranker, and Elizabeth Rhoades**

Islet amyloid polypeptide (IAPP, also known as amylin) is a 37-residue peptide hormone co-secreted with insulin by pancreatic β cells. IAPP is natively unstructured, but gains α-helical structure on binding to anionic membranes[1] and forms β-sheet-rich amyloid fibers during the progression of type II diabetes.[2] Membrane disruption by nonfibrillar α-helical oligomers of IAPP has been implicated in β-cell death and dysfunction.[3] Anionic membranes also dramatically accelerate the formation of IAPP fibrils,[4] possibly by favoring an oligomeric nucleating state. Therefore, membrane-bound states of IAPP are of significant interest.[5] Lipid-bound monomeric IAPP has been structurally characterized at high resolution,[6,7] but oligomers are dynamic, heterogeneous, and transient, thus presenting a challenge for traditional structure determination approaches. Several research groups have studied these oligomeric states,[8,9] but fundamental questions about their topology and stoichiometry remain.

We approached this problem by using intermolecular single-pair Förster resonance energy transfer (spFRET) measurements to selectively study membrane-bound IAPP oligomers from a predominantly monomeric population. To avoid experimental complications arising from fiber formation, we used the rat isoform of IAPP (rIAPP), which differs from the human isoform (hIAPP) in six residues. Similar to hIAPP, rIAPP can cause membranes to become permeable[10] and causes cell toxicity,[11] but it does not form amyloid.[12] The rIAPP was labeled with either a single donor (Alexa 488) at one of five residues, or an acceptor (Atto 610) at residue 1 (Figure 1). Measurements were made in a dilute mixture of labeled rIAPP and 1,2-dioleoyl-*sn*-glycero-3-[phospho-*rac*-(1-glycerol)] (DOPG) nanodiscs[13] as the particles diffused through a focused laser beam. The energy-transfer efficiency (ET_{eff}) was calculated for each transit of a fluorescent particle through the focal volume. Energy transfer only occurs when at least one donor-labeled and one acceptor-labeled rIAPP are bound to the same nanodisc (see Figure S1c in the Supporting Information). Intramolecular spFRET using double-labeled rIAPP served to verify the expected conversion from a compact disordered state in solution to a helical state in the presence of membranes (Figure 1F).

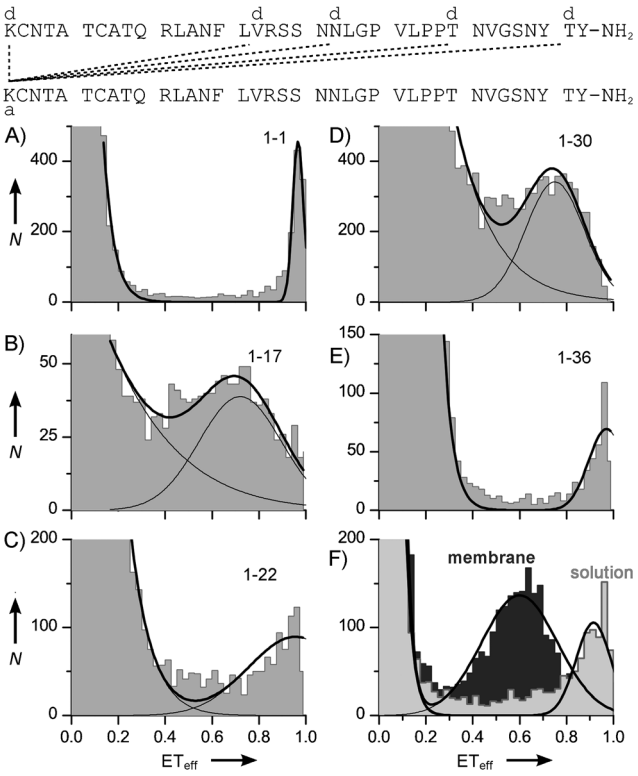

Figure 1. A–E) spFRET histograms collected from a mixture of rIAPP, separately labeled with donor (d) or acceptor (a) at the positions indicated, and nanodiscs. A small fraction of rIAPP forms membrane-bound dimers, and the minor species ET_{eff} peak reports on the dimer structure. F) SpFRET of rIAPP, double-labeled at residues 1 and 36, in solution (light gray) and on membranes (dark gray). If IAPP formed a parallel membrane-bound dimer, the intermolecular ET_{eff} value for the 1–36 residue pair (panel E) would more closely match the latter intramolecular value (ca. 0.6).

Under our experimental conditions, we expected rIAPP to be largely monomeric (free in solution or membrane-bound) as reflected by the major peak centered at $ET_{eff} = 0$ in all histograms (Figure 1A–E). A minor but significant population of events with $ET_{eff} > 0.25$ (ca. 0.5%) results from nanodiscs containing at least one donor–acceptor rIAPP pair. Residue pairs 1–36 and 1–1 displayed the highest peak ET_{eff}, followed by 1–22, 1–30, and 1–17. As an

[*] Dr. A. Nath, Prof. A. D. Miranker, Prof. E. Rhoades
Molecular Biophysics & Biochemistry, Yale University
New Haven CT 06520-8114 (USA)
E-mail: andrew.miranker@yale.edu
elizabeth.rhoades@yale.edu

[**] This work was funded by an American Heart Association Postdoctoral Fellowship for A.N. and NIH grant GM-084391 to E.R. and A.D.M. We thank Dr. S. G. Sligar (UIUC) for the gift of MSP1D1, Y. Gofman of the Ben-Tal group (Tel Aviv University) for assistance with MCPep, Dr. J. Knight, Dr. T. Craggs, and Dr. C. J. Wilson for critical reading, J. Dunn for expressed IAPP, the W. M. Keck Biotechnology Research Laboratory for peptide synthesis, and the Yale FAS High Performance Computing Center.

Supporting information for this article is available on the WWW under http://dx.doi.org/10.1002/anie.201102887.

orthogonal probe of inter-rIAPP contacts, chemical cross-linking showed approximately the same reactivity as the spFRET data (see Figure S1b in the Supporting Information). However, this ensemble assay required much higher protein and lipid concentrations than spFRET, and consequently reports on a more heterogeneous population of oligomers. In the absence of nanodiscs, the high ET_{eff} population is not observed, consistent with the expectation that rIAPP is monomeric in solution at low concentrations (see Figure S1d in the Supporting Information). Importantly, bacterially expressed IAPP provides a similarly high ET_{eff} population to the synthesized peptide (see Figure S1e in the Supporting Information), which indicated that these events do not represent a contaminating sub-population from the peptide synthesis. Data obtained by using several techniques, including fluorescence, gel filtration chromatography, and cross-linking, suggest that an IAPP dimer is a favorable oligomeric state in solution and on membranes, where it is the dominant oligomer at low protein/lipid ratios.[4,14] Doubling the amount of donor-labeled rIAPP increased the high ET_{eff} population by a factor of two, as expected for a dimer rather than a higher-order oligomer (see Figure S1f in the Supporting Information). The fraction of high ET_{eff} events (ca. 0.5%) is significantly higher than would be expected if rIAPP were to bind nanodiscs without self-association (ca. 0.02%; see the Supporting Information for details). Thus, while another highly favored complex may exist, a dimer is statistically the most probable oligomer at the low concentrations used for spFRET and the simplest model which is consistent with the data.

Assuming that high ET_{eff} peak positions report on a dimer structure, the peaks obtained show that residue 1 of one monomer is relatively close to residues 1 and 36 of the other and far from residues 17 and 30. These data rule out a parallel, in-register, coiled coil. Given that the dyes and linker moieties are large relative to systems such as IAPP dimers, a solely qualitative analysis of these data is inadequate. Therefore, we used Rosetta[15] to generate stable models of rIAPP dimers which were consistent with the spFRET data (see the Supporting Information for details). The flexible linkers for attaching dyes to proteins can add up to 15.7 Å (Alexa 488) and 10.1 Å (Atto 610) to ET_{eff}-derived distances (see Figure S2 in the Supporting Information). Therefore, each spFRET constraint was considered satisfied if the difference between the inter-dye distance (calculated from ET_{eff} and the Förster equation) and the C_α–C_α distance was less than the sum of these average dye–C_α distances. Harmonic potentials were applied to distances outside of these broad boundaries.

While unconstrained refinement produced both parallel and antiparallel topologies of comparable energy, spFRET constraints strongly biased the search towards three similar conformations. The favored conformations were dimers interacting through a short (ca. 5 turns) antiparallel coiled-coil motif, with the flexible tails oriented so that the N and C termini of a given monomer were approximately equidistant from the N-terminus of the other monomer (Figure 2). The low-energy models obtained by the constrained search are also compatible with NMR-derived secondary structure assignments of membrane-bound, monomeric rIAPP.[16] The

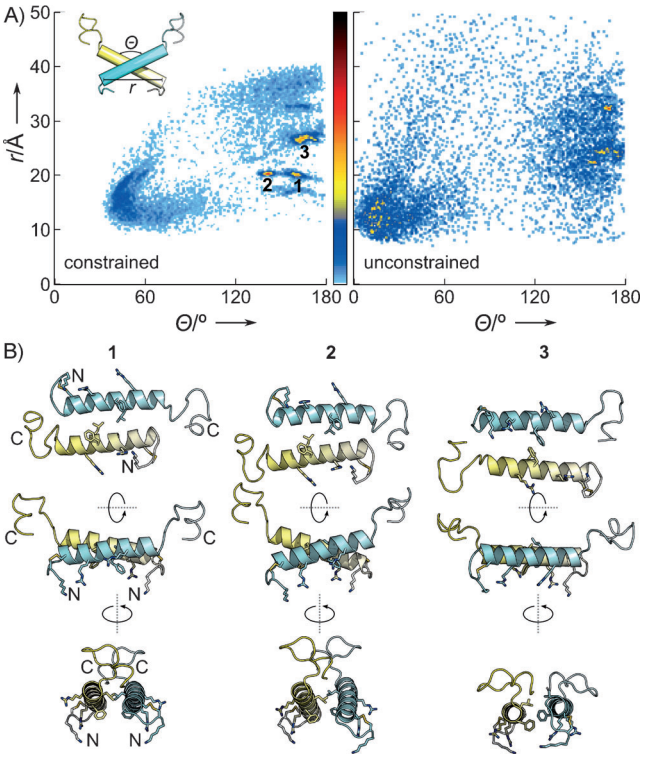

Figure 2. A) rIAPP dimer models generated by constrained (left) and unconstrained (right) docking. These are plotted in terms of distance between the N-terminal ends of the two helices *r* vs. interhelical angle, *θ*. B) Detailed views of representatives from each cluster, perpendicular to (top) and in the plane of (middle, bottom) the membrane. Side chains proposed to participate in dimerization and membrane binding are shown as sticks.

spFRET constraints were self-consistent and narrowed the search space progressively as additional constraints were applied. Importantly, randomized constraints failed to generate a stable structure (see Figure S3 in the Supporting Information).

Constrained dimer models had a dimer interface involving residues L12, F15, and L16. These displayed a very plausible lipid-binding interface, even though the simulations did not include a membrane: residues A5, A8, L12, F15, and L23 form a central hydrophobic patch; charged residues K1, R11, and R18 are free to interact with anionic head groups; and flexible C-terminal tails are exposed to solution. The resulting orientation in the plane of the membrane resembles the orientation predicted by MCPep[17] as the expected binding mode of an amphipathic helical peptide like IAPP (see Figure S4 in the Supporting Information). The dimer interface corresponds well to self-assembly sequences suggested by others.[18] Compared with proposed models of hIAPP and rIAPP dimers in the gas phase (in the absence of solvent or a membrane),[19] our results indicate an increase in helical structure and a stronger preference for antiparallel arrangements. An antiparallel dimer also differs from the crystal structure of IAPP fused to the 370-residue maltose-binding protein (MBP),[20] again in the absence of a membrane, which shows a helix–helix dimer with a similar hydrophobic interface, but a 55° interhelix angle. The differences between these

various dimer models might reflect the crucial role that environment and, in particular, membranes, can play in controlling IAPP conformation. We note that if IAPP has both a preferred membrane-binding face and a symmetric dimer interface, then purely geometric considerations require an antiparallel topology for a membrane-bound dimer. The spFRET-constrained models satisfy this requirement, whereas a parallel dimer would imply either an asymmetric dimer interface or different membrane-binding orientations for the two monomers.

The peptide sequences of hIAPP and rIAPP differ at six residues, one (position 18) located in the membrane-binding region and the other five in the flexible C terminus. The structures of both membrane-bound monomers are known to be broadly similar,[1,6] and none of these residues form part of the dimer interface in the low-energy antiparallel models. All of the favorable interactions involved in maintaining the rIAPP dimer are also available for similar self-association with hIAPP, which suggests that hIAPP may also form an antiparallel helix–helix dimer. This possibility is especially intriguing given that fibrils show a parallel arrangement.[7,9] If this is the case for hIAPP, then either the analogous antiparallel hIAPP dimer would represent a low-energy, off-pathway species, or the amyloidogenic pathway must include a transition from a previously unanticipated antiparallel arrangement to a parallel one. Stabilization of an antiparallel dimer could, in either case, inhibit further oligomerization and subsequent pathology, building on previous small-molecule designs that deliberately target the α-helical surface of IAPP.[21]

The spFRET technique proved uniquely well-suited to dissecting the heterogeneity inherent in cooperative membrane binding by rIAPP, by distinguishing membrane-bound dimers from the predominant monomeric species. The spFRET-constrained Rosetta calculations (to our knowledge, the first combined application of these powerful techniques) found a population of low-energy, antiparallel helix–helix dimers that satisfy all the spFRET restraints. These dimers appear competent for membrane binding and agree with other reports on homodimeric interaction interface of IAPP. The models presented here are the most detailed yet proposed for a membrane-bound rIAPP oligomer. Future studies will extend this method to hIAPP and focus on subsequent states in the oligomerization pathway, including those which disrupt membrane integrity.[10] We will also study the possible effects of more physiological, heterogeneous membrane compositions in modulating IAPP conformation. More generally, the combination of spFRET and high-resolution refinement may prove useful in the study of other unstructured, toxic, amyloid-forming peptides and proteins, including amyloid-β, α-synuclein, tau, and prion protein.[3,22]

Experimental Section

Donor (Alexa 488) and acceptor (Atto 610) dyes were attached to mutant peptides that were synthesized with an alkyne group at residues 17, 22, 30, or 36, by using click chemistry, or by an amine coupling to residue 1. Nanodiscs were prepared as previously described.[13] Confocal spFRET was performed on mixtures of donor-labeled peptide (100 pM), acceptor-labeled peptide (500 pM), and DOPG nanodiscs (40 nM) as previously described.[13] Cross-linking was performed between azide-labeled rIAPP at residue 1 and the four alkyne-bearing mutants by using click chemistry. Constrained dimer model refinement was implemented in Rosetta as detailed in the Supporting Information.

Received: April 27, 2011
Revised: July 27, 2011
Published online: September 22, 2011

Keywords: amyloid · molecular modeling · oligomerization · peptides · single-molecule studies

[1] J. A. Williamson, J. P. Loria, A. D. Miranker, *J. Mol. Biol.* **2009**, *393*, 383 – 396.
[2] P. Westermark, C. Wernstedt, E. Wilander, D. W. Hayden, T. D. O'Brien, K. H. Johnson, *Proc. Natl. Acad. Sci. USA* **1987**, *84*, 3881 – 3885.
[3] a) J. A. Hebda, A. D. Miranker, *Annu. Rev. Biophys.* **2009**, *38*, 125 – 152; b) A. Abedini, D. P. Raleigh, *Protein Eng. Des. Sel.* **2009**, *22*, 453 – 459.
[4] J. D. Knight, J. A. Hebda, A. D. Miranker, *Biochemistry* **2006**, *45*, 9496 – 9508.
[5] J. R. Brender, E. L. Lee, M. A. Cavitt, A. Gafni, D. G. Steel, A. Ramamoorthy, *J. Am. Chem. Soc.* **2008**, *130*, 6424 – 6429.
[6] a) S. M. Patil, S. Xu, S. R. Sheftic, A. T. Alexandrescu, *J. Biol. Chem.* **2009**, *284*, 11982 – 11991; b) R. P. Nanga, J. R. Brender, J. Xu, K. Hartman, V. Subramanian, A. Ramamoorthy, *J. Am. Chem. Soc.* **2009**, *131*, 8252 – 8261; c) R. P. Nanga, J. R. Brender, S. Vivekanandan, A. Ramamoorthy, *Biochim. Biophys. Acta Biomembr.* **2011**, *1808*, 2337 – 2342.
[7] a) S. Luca, W. M. Yau, R. Leapman, R. Tycko, *Biochemistry* **2007**, *46*, 13505 – 13522; b) S. A. Jayasinghe, R. Langen, *J. Biol. Chem.* **2004**, *279*, 48420 – 48425.
[8] a) R. Mishra, M. Geyer, R. Winter, *ChemBioChem* **2009**, *10*, 1769 – 1772; b) R. Soong, J. Brender, P. M. Macdonald, A. Ramamoorthy, *J. Am. Chem. Soc.* **2009**, *131*, 7079 – 7085; c) F. Evers, C. Jeworrek, S. Tiemeyer, K. Weise, D. Sellin, M. Paulus, B. Struth, M. Tolan, R. Winter, *J. Am. Chem. Soc.* **2009**, *131*, 9516 – 9521; d) S. Jha, D. Sellin, R. Seidel, R. Winter, *J. Mol. Biol.* **2009**, *389*, 907 – 920; e) Y. L. Ling, D. B. Strasfeld, S. H. Shim, D. P. Raleigh, M. T. Zanni, *J. Phys. Chem. B* **2009**, *113*, 2498 – 2505; f) R. Kayed, J. Bernhagen, N. Greenfield, K. Sweimeh, H. Brunner, W. Voelter, A. Kapurniotu, *J. Mol. Biol.* **1999**, *287*, 781 – 796.
[9] L. Fu, G. Ma, E. C. Yan, *J. Am. Chem. Soc.* **2010**, *132*, 5405 – 5412.
[10] N. B. Last, E. Rhoades, A. D. Miranker, *Proc. Natl. Acad. Sci. USA* **2011**, *108*, 9460 – 9465.
[11] M. Magzoub, A. D. Miranker, unpublished results.
[12] M. Nishi, S. J. Chan, S. Nagamatsu, G. I. Bell, D. F. Steiner, *Proc. Natl. Acad. Sci. USA* **1989**, *86*, 5738 – 5742.
[13] A. Nath, A. J. Trexler, P. Koo, A. D. Miranker, W. M. Atkins, E. Rhoades, *Methods Enzymol.* **2010**, *472*, 89 – 117.
[14] a) E. Andreetto, L. Yan, M. Tatarek-Nossol, A. Velkova, R. Frank, A. Kapurniotu, *Angew. Chem.* **2010**, *122*, 3146 – 3151; *Angew. Chem. Int. Ed.* **2010**, *49*, 3081 – 3085; b) L. M. Yan, M. Tatarek-Nossol, A. Velkova, A. Kazantzis, A. Kapurniotu, *Proc. Natl. Acad. Sci. USA* **2006**, *103*, 2046 – 2051.
[15] a) C. A. Rohl, C. E. Strauss, K. M. Misura, D. Baker, *Methods Enzymol.* **2004**, *383*, 66 – 93; b) S. Chaudhury, S. Lyskov, J. J. Gray, *Bioinformatics* **2010**, *26*, 689 – 691; c) K. W. Kaufmann, G. H. Lemmon, S. L. Deluca, J. H. Sheehan, J. Meiler, *Biochemistry* **2010**, *49*, 2987 – 2998.

[16] J. Williamson, A. Miranker, *Protein Sci.* **2007**, *16*, 110 – 117.
[17] D. Shental-Bechor, T. Haliloglu, N. Ben-Tal, *Biophys. J.* **2007**, *93*, 1858 – 1871.
[18] a) R. Azriel, E. Gazit, *J. Biol. Chem.* **2001**, *276*, 34156 – 34161; b) A. Fox, T. Snollaerts, C. Errecart Casanova, A. Calciano, L. A. Nogaj, D. A. Moffet, *Biochemistry* **2010**, *49*, 7783 – 7789.
[19] a) N. F. Dupuis, C. Wu, J. E. Shea, M. T. Bowers, *J. Am. Chem. Soc.* **2009**, *131*, 18283 – 18292; b) N. F. Dupuis, C. Wu, J. E. Shea, M. T. Bowers, *J. Am. Chem. Soc.* **2011**, *133*, 7240 – 7243.
[20] J. J. Wiltzius, S. A. Sievers, M. R. Sawaya, D. Eisenberg, *Protein Sci.* **2009**, *18*, 1521 – 1530.
[21] J. A. Hebda, I. Saraogi, M. Magzoub, A. D. Hamilton, A. D. Miranker, *Chem. Biol.* **2009**, *16*, 943 – 950.
[22] a) S. Elbaum-Garfinkle, T. Ramlall, E. Rhoades, *Biophys. J.* **2010**, *98*, 2722 – 2730; b) M. Morillas, W. Swietnicki, P. Gambetti, W. Surewicz, *J. Biol. Chem.* **1999**, *274*, 36859 – 36865.

